

Competitive Polymerization between Organic and Inorganic Networks in Hybrid Materials

Plinio Innocenzi* and Giovanna Brusatin

*Dipartimento di Ingegneria Meccanica, Settore Materiali, Università di Padova,
via Marzolo 9, 35131 Padova, Italy*

Florence Babonneau

*Chimie de la Matière Condensée, Université Paris 6-T54-E5, 4 place Jussieu,
75252 Paris Cedex 05, France*

Received July 21, 2000. Revised Manuscript Received September 21, 2000

Hybrid organic–inorganic materials derived from 3-glycidoxypropyltrimethoxysilane have been synthesized via sol–gel using BF_3 etherate as a catalyst of organic polymerization. Different amounts of BF_3 etherate have been used, from $\text{B/Si} = 0.01$ up to $\text{B/Si} = 0.1$, to prepare powder samples. The materials have been characterized by Fourier transform infrared spectroscopy (FTIR) and multinuclear solid-state NMR spectroscopy. FTIR and NMR spectra have shown that with a $\text{B/Si} = 0.03$ molar ratio a complete opening of epoxy in 3-glycidoxypropyltrimethoxysilane is achieved. The different amounts of BF_3 etherate employed have been found to affect the degree of inorganic cross-linking and the length of the ethylene oxide chains. Larger amounts of BF_3 enhance the inorganic network cross-linking and give oligo(ethylene oxide) derivatives. Boron has been found to remain in the matrix as a network former of the inorganic side. The formation of Si–O–B bonds has been observed by the FTIR spectra.

Introduction

An important class of organic–inorganic materials is represented by 3-glycidoxypropyltrimethoxysilane (GPTMS) derived hybrids.^{1–5} In these materials organic and inorganic units are linked together via covalent bonds while the presence in GPTMS of an epoxy ring, which can be a former of organic polymers, allows the buildup of a polymeric network. The organic polymerization is simultaneously achieved with the formation of the inorganic network.

Epoxy groups react to form poly(ethylene oxide) (PEO) chains via photo- or thermal⁶-induced polymerization or via basic^{7,8} or acid catalysts.^{1,5} The oxiranes can also react with water in acidic conditions or with methanol to form diols or methyl ether terminal groups.⁹ Examples of basic catalysts are 1-methylimidazole^{7,10} (MI) and (γ -aminopropyl)triethoxysilane⁸ (APTES). These compounds act at the same time as catalysts of the siloxane polymerization and initiators of organic po-

lymerization. MI is an efficient catalyst of epoxy ring opening but, however, does not contribute directly to the formation of the network. APTES, which is a trifunctional silane, instead, participates also in the formation of the network, which will be ultimately modified by amino functions.

Lewis acids, such as titanium,^{11,2} zirconium,^{12,2} or aluminum alkoxides,⁹ are also efficient initiators of organic polymerization. These alkoxides, cohydrolyzed, with GPTMS will be incorporated into the silicon-based inorganic network. The final properties of these hybrid materials are, in this case, strongly dependent on the catalyst of epoxy reactions.

Another example of a compound that can be used in the synthesis of GPTMS-derived hybrid materials is BF_3 etherate. In a previous paper¹³ we reported a new synthesis route of GPTMS hybrids from BF_3 . This synthesis has the advantage of requiring lower temperatures and preparation times and giving very homogeneous materials. This hybrid matrix has been used as a host for fullerene derivatives to fabricate an optical limiting device:^{14,15} a very fine dispersion of fullerene derivatives can be obtained in this matrix and a larger laser damage threshold is reached with respect to other

* To whom correspondence should be addressed.

- (1) Schmidt, H. *J. Non-Cryst. Solids* **1985**, *73*, 681.
- (2) Philipp, G.; Schmidt, H. *J. Non-Cryst. Solids* **1986**, *82*, 31.
- (3) Schmidt, H. *J. Non-Cryst. Solids* **1989**, *112*, 419.
- (4) Nass, R.; Arpac, E.; Glaubitt, W.; Schmidt, H. *J. Non-Cryst. Solids* **1990**, *121*, 370.
- (5) Schmidt, H. *J. Non-Cryst. Solids* **1994**, *178*, 302.
- (6) Kasemann, R.; Bruck, S.; Schmidt, H. *SPIE* **1994**, *2288*, 321.
- (7) Popall, M.; Durand, H. *Electrochim. Acta* **1992**, *37*, 1593.
- (8) Riegel, B.; Blittersdorf, S.; Kiefer, W.; Hofacker, S.; Muller, M.; Schottner, G., *J. Non-Cryst. Solids* **1998**, *226*, 76.
- (9) Templin, M.; Wiesner, U.; Spiess, H. W. *Adv. Mater.* **1997**, *9*, 814.
- (10) Kasemann, R.; Schmidt, H. *Proceedings First European Workshop on Hybrid Organic–Inorganic Materials*, Sanchez, C., Ribot, F., Eds.; Chateau de Bierville: France, 1993; p 171.

(11) Hoebbel, D.; Nacken, M.; Schmidt, H. *J. Sol–Gel Sci. Technol.* **1998**, *12*, 169.

(12) Sorek, Y.; Zevin, M.; Reisfeld, R.; Hurvits, T.; Rushin, S. *Chem. Mater.* **1997**, *9*, 670.

(13) Innocenzi, P.; Brusatin, G.; Guglielmi, M.; Bertani, R. *Chem. Mater.* **1999**, *11*, 1672.

(14) Brusatin, G.; Innocenzi, P.; Guglielmi, M.; Bozio, R.; Meneghetti, M.; Signorini, R.; Maggini, M.; Scorrano, G.; Prato, M. *SPIE* **1999**, *3803*, 90.

hybrid systems prepared with zirconium or titanium alkoxides. BF_3 can also promote the inorganic polymerization to a larger extent compared to other metal alkoxides.¹³

An important point in the synthesis of this class of hybrids is related to the effect on the PEO chain lengths of the simultaneous organic and inorganic polymerization. The two processes, if not carefully controlled, are in competition. If the silica network is formed much faster than the organic polymer, the organic chains cannot find enough space to grow and their length is greatly reduced. Because of the strong effect of BF_3 on both polymerization processes, the inorganic and organic one, we have used the synthesis reported in the previous paper to study the network formation as a function of the amount of catalyst. The objective was to understand how the microstructure is affected by these competitive processes.

Experimental Section

Materials. Tetraethyl orthosilicate, (3-glycidioxypropyl)-trimethoxysilane, and boron trifluoride diethyl etherate (Aldrich) were all analytical grade and purchased from Aldrich. Bidistilled water for hydrolysis of alkoxides and HCl (1 N) as the catalyst were used. Methyl alcohol (Prolabo), analytical grade, was the solvent.

Synthesis of the Precursor Sol. The precursor sol was prepared by using a precondensation reaction, done under reflux at 80 °C for 4 h, where GPTMS and TEOS were cohydrolyzed, under acidic conditions with HCl as the catalyst and methyl alcohol (MeOH) as the solvent. The molar ratios between the reagents were $(\text{GPTMS}/\text{TEOS}) = 7:3$ and $(\text{GPTMS} + \text{TEOS})/\text{H}_2\text{O}/\text{HCl}/\text{MeOH} = 1:3.3:0.004:0.013$. This buffer sol will be indicated as GTB0.

Different sols were prepared by adding to GT different amounts of BF_3OEt_2 , with molar ratios with respect to Si of 1% (GTB1), 2% (GTB2), 3% (GTB3), 5% (GTB5), and 10% (GTB10). The sols were diluted by adding the proper amount of BF_3OEt_2 together with methyl alcohol $(\text{GPTMS} + \text{TEOS}/\text{MeOH}) = 1:8$. After the addition of BF_3OEt_2 , the sols were stirred for 1 h at room temperature before using.

Sample Preparation. Powders were prepared from solutions poured into Petri dishes and maintained in a thermostatic chamber at 60 °C for 24 h.

Elemental Analysis. The elemental analyses have been performed by the Service Central d'Analyse du CNRS, Verneuil, France.

NMR Characterization. The ^{29}Si and ^{13}C solid state NMR spectra have been recorded with a MSL300 Bruker spectrometer at respectively 59.63 and 75.47 MHz using a CP-MAS Bruker probe equipped with 7-mm ZrO_2 rotors, spinning at 4 kHz. The following acquisition parameters were used for ^{29}Si : spectral width of 20 kHz, 2 K data points, pulse width of 2 μs ($\theta \approx 30^\circ$), and recycle delay of 60 s. Exponential broadening, 50 Hz, was applied before Fourier transform. The Si units from GPTMS and TMOS will be labeled respectively T_i and Q_i , i representing the number of oxobridges surrounding the central Si atom.¹⁶ The ^{13}C CP MAS NMR spectra were recorded under the same Hartmann–Hahn match condition, set up by using a powdered sample of adamantane: both RF channel levels $\omega_{1\text{H}}/2\pi$ and $\omega_{13\text{C}}/2\pi$ were adjusted so that $|\omega_{1\text{H}}/2\pi| = |\omega_{13\text{C}}/2\pi| = 43$ kHz. Proton decoupling was applied during acquisition.

(15) (a) Signorini, R.; Meneghetti, M.; Bozio, R.; Maggini, M.; Scorrano, G.; Prato, M.; Brusatin, G.; Innocenzi, P.; Guglielmi, M. *Carbon* **2000**, *38*, 1653. (b) Innocenzi, P.; Brusatin, G.; Guglielmi, M.; Signorini, R.; Meneghetti, M.; Bozio, R.; Maggini, M.; Scorrano, G.; Prato, M. *J. Sol-Gel Sci. Technol.* **2000**, *19*, 263. (c) Innocenzi, P.; Brusatin, G.; Guglielmi, M.; Signorini, R.; Bozio, R.; Maggini, M. *J. Non-Cryst. Solids* **2000**, *265*, 68.

(16) Williams, E. A. *Annu. Rep. NMR Spectrosc.* **1983**, *15*, 235.

Table 1. Elemental Analysis of the Powders (B and Si Content)

sample	B (wt %)	Si (wt %)	B/Si (molar ratio) measured value	B/Si (molar ratio) nominal value
GTB10	0.61	15.00	0.100	0.10
GTB5	0.23	15.30	0.038	0.05
GTB3	0.14	16.70	0.022	0.03
GTB2	0.14	17.90	0.020	0.02
GTB1	0.10	16.95	0.015	0.01

A contact time of 3 ms was used, with a spectral width of 20 kHz and 1 K data points. Exponential broadening, 20 Hz, was applied before Fourier transform. ^{29}Si and ^{13}C NMR spectra were referenced externally to TMS at 0 ppm. The ^{11}B MAS NMR spectra were recorded with a MSL400 Bruker spectrometer at 128.28 MHz using a CP-MAS Doty probe equipped with 5-mm Si_3N_4 rotors, spinning at 9–10 kHz. The following acquisition parameters were used: spectral width of 50 kHz, 4 K data points, pulse width of 0.7 μs , and a recycle delay of 1 s. Proton decoupling was applied during acquisition and 50-Hz exponential broadening was applied before Fourier transform. Spectra were referenced externally to $(\text{OEt})_2\text{BF}_3$ at 0 ppm. The experimental spectra were simulated by using the WinFit software developed by D. Massiot et al.¹⁷

Infrared Spectroscopy. Infrared absorption spectra in the range 6500–400 cm^{-1} were recorded by Fourier transform infrared spectroscopy (FTIR) (Perkin–Elmer 2000), with a resolution of ± 1 cm^{-1} , on powders using anhydrous KBr as the pellet.

Results

Elemental analysis. The results of elemental analysis on the various powdered samples are reported in Table 1. A good agreement is found between nominal and measured B/Si molar ratios. Boron remains in the samples to a large extent with respect to the nominal amount.

FTIR Spectra. The absorption IR spectra of epoxides show four characteristic bands^{18,19} at 1260–1240 (ring breathing), 950–810 cm^{-1} (asymmetrical ring stretching), 865–785 cm^{-1} (unassigned), and 3050–2995 cm^{-1} (C–H stretch in the epoxide). The band in the range 3050–2995 cm^{-1} , which does not overlap with any other absorption band, was taken as a reference to obtain a semiquantitative evaluation of the epoxy ring content in the samples. Figure 1 shows the FTIR normalized spectra of the samples synthesized with different amounts of BF_3 . GTB5 and GTB10 do not show any more this absorption due to the epoxy groups. This band is very weak in GTB3 and more intense in GTB2 and GTB1.

Figure 2 shows the FTIR absorption spectra of the GTB $_x$ ($x = 1, 2, 3, 5, 10$) samples between 940 and 820 cm^{-1} . The bands at 910 and 855 cm^{-1} , assigned to the epoxy groups, decrease with larger boron contents, while a new band at 890 cm^{-1} is detected with an opposite trend, which is attributed to the formation of Si–O–B bonds in the network.

An intense band around 1100 cm^{-1} is detected in the FTIR spectra of all the samples and is attributed to the asymmetric stretching vibration of Si–O–Si bonds.²⁰

(17) Massiot, D.; Thiele, H.; Germanus, A. *Bruker Rep.* **1994**, *140*, 43.

(18) *Comprehensive Heterocyclic Chemistry*; Lwoswski, W., Ed.; Pergamon Press: Oxford, U.K., 1984; Vol. 7, p 99.

(19) *Atlas of Spectral Data and Physical Constants for Organic Compounds*; Grasselli, J. G., Ritchey, W. M., Eds.; CRC Press Inc.: Cleveland, OH, 1975; Vol. 1.

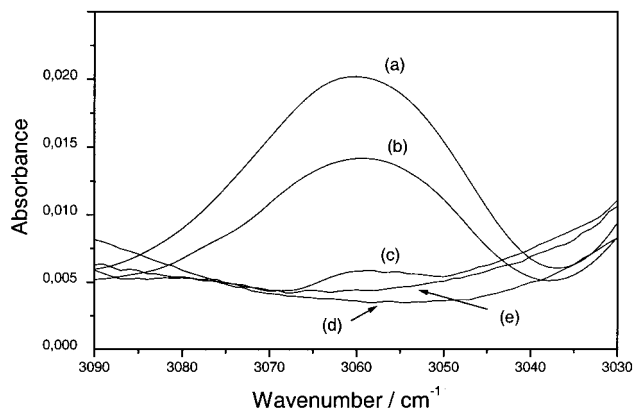


Figure 1. FTIR normalized spectra of GTB1 (a), GTB2 (b), GTB3 (c), GTB5 (d), and GTB10 (e) around 3060 cm^{-1} (C-H epoxy stretch).

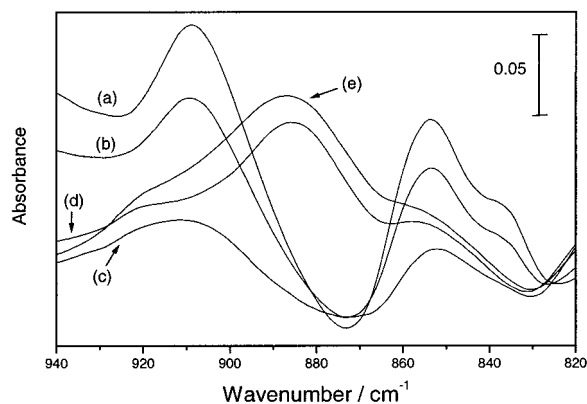


Figure 2. FTIR normalized spectra of GTB1 (a), GTB2 (b), GTB3 (c), GTB5 (d), and GTB10 (e) around 880 cm^{-1} (asymmetrical epoxy ring stretching at $\approx 910\text{ cm}^{-1}$, Si-O-B band at $\approx 855\text{ cm}^{-1}$, and epoxy band at $\approx 850\text{ cm}^{-1}$).

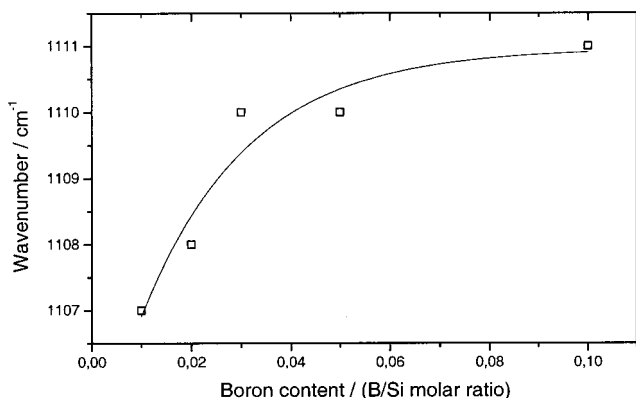


Figure 3. Peak position of the infrared Si-O-Si band around 1100 cm^{-1} as a function of boron content (B/Si molar ratio) with respect to the nominal composition. The line is a guide for eyes.

The position of this band is shown in Figure 3 as a function of the boron content: a shift to higher wavenumbers with the increase in boron is observed.

NMR Spectra. ^{13}C CP MAS NMR Spectra. Figure 4 shows the ^{13}C CP MAS NMR spectra of the samples with different boron contents. For comparison, the spectrum of a sample prepared without boron (GTB0) is also presented. The assignments of the peaks, dis-

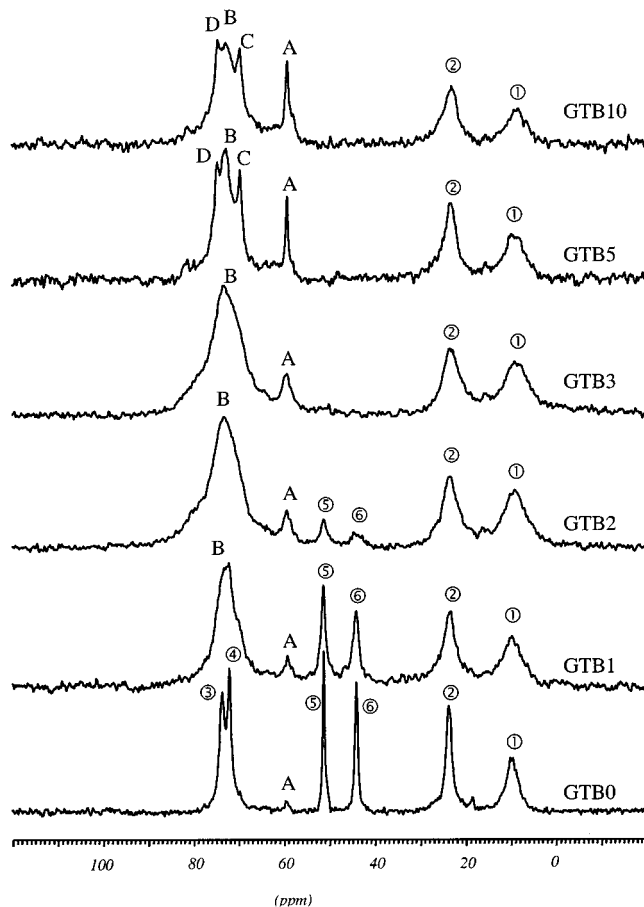


Figure 4. ^{13}C CP MAS NMR spectra of the samples prepared with different amounts of BF_3 .

cussed in the following section, are summarized in Table 2. The signals due to the carbon atoms in the GPTMS molecules (labeled from 1 to 6 in Scheme 1) can be recognized in the spectrum of GTB0, especially those due to the epoxy rings at 44 ppm (6) and 51 ppm (5).

In GTB1, these peaks are still sharp and intense; they show a strong reduction in intensity in GTB2, while for $\text{B/Si} \geq 0.03$, they are no longer observed, indicating total completion of the ring-opening reaction. The decrease in intensity of these peaks is directly related to the appearance of a broad and intense peak around 74 ppm (B) (Figure 4b-d). This chemical shift value is characteristic of C atoms in oligo- or poly(ethylene oxide) derivative species formed from a ring-opening reaction of the epoxy groups⁹ (Scheme 2).

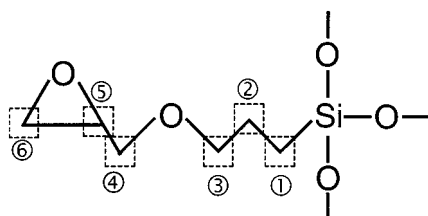
For $\text{B/Si} < 0.03$, the observed peak is certainly due to the overlap of signals due to unpolymerized and polymerized species. For $\text{B/Si} \geq 0.05$, the shape of this signal changes with the presence of two new resolved peaks at 70 ppm (C) and 75 ppm (D). The sharpening of the peaks due to the $\text{CH}_x\text{-O}$ species ($x = 1$ and 2) may indicate the presence of shorter poly(ethylene oxide) derivative chains for the highest B contents.

One peak is also present at 59 ppm (A), whose intensity increases from GTB1 to GTB10. This signal is attributed to carbon atoms in a methyl ether terminal group⁹ (Scheme 3).

It is interesting to see that the line width of this peak follows an evolution similar to that of the signals around 70–75 ppm: for $\text{B/Si} \geq 0.05$, this peak strongly sharpens, suggesting a higher mobility for these terminal

Table 2. Assignment of the Signals in the ^{13}C CP MAS NMR Spectra of the Samples GTB x ($x = 1, 2, 3, 5, 10$) (The Labels Used To Indicate the Signals in Figure 4 Are Also Reported; Labels from 1 to 6 Refer to Carbons in GPTMS, while Peaks from A to D Refer to Units Formed after Reaction of GPTMS)

chemical shift (ppm)	units	comments	label
≈ 10	$\equiv\text{Si}-\text{CH}_2-\text{CH}_2-$	first carbon atom close to the silicon	1
≈ 24	$\equiv\text{Si}-\text{CH}_2-\text{CH}_2-$	second carbon atom close to the silicon	2
≈ 75	$-\text{CH}_2-\text{CH}_2-\text{O}-\text{CH}_2-$	carbon in the ether bridge of GPTMS	3
≈ 73	$-\text{CH}_2-\text{CH}_2-\text{O}-\text{CH}_2-$	carbon in the ether bridge of GPTMS	4
≈ 51	$\text{CH}_2(-\text{O})-\text{CH}-$	carbon in the epoxy ring	5
≈ 44	$\text{CH}_2(-\text{O})-\text{CH}-$	carbon in the epoxy ring	6
≈ 59	$-\text{O}-\text{CH}_2-\text{C}(\text{OH})-\text{CH}_2-\text{O}-\text{CH}_3$	terminal methyl ether group	A
$\approx 70-75$	$-\text{O}-\text{CH}_2-[-\text{CH}_2-\text{CH}_2-]_n-\text{O}-$	carbons in the poly(ethylene oxide) chain	B, C, D

Scheme 1

species. A peak at 64 ppm due to the formation of diol functions according to the reaction presented in Scheme 4 is not clearly seen in these series of spectra, suggesting that this reaction, if occurring, is a minor one.

The peaks at 10 ppm (1) and 24 ppm (2), assigned to the carbon atoms close to the silicon one, in positions 1 and 2, respectively, are also sensitive to the organic polymerization reactions. Their line widths increase with boron content, as a result of a larger distribution of C sites due to an increase in network rigidity.

^{29}Si MAS NMR Spectra. Figure 5 shows the ^{29}Si MAS NMR spectra of the samples GTB x with signals around -110 and -100 ppm due to Q_4 and Q_3 units (from TEOS) and around -65 and -60 ppm due to T_3 and T_2 units (from GPTMS). One can observe a broadening of the T units as soon as B is introduced in the network, similar to what was just observed for the ^{13}C signals of C sites 1 and 2. This may also be attributed to an increase in the network rigidity because of an increase in cross-linking. The spectra were simulated to extract the relative amounts of T and Q units (Table 3). Because of a strong overlap between the T_2 and T_3 signals, the simulations may not be very precise for the T units, but they show clear trends in the evolution of the extent of condensation of the various units. They show first that the $T:Q$ molar ratio in the various gels corresponds to the GPTMS:TEOS ratio introduced in the starting solution (70:30). With increasing boron contents, the degree of condensation of each type of units increases, and this effect is more pronounced for Q units than for T units. The chemical shift values for the various units present some variations (about 2 ppm), depending on the sample composition that might be related to the introduction of B but no clear conclusions can be given.

^{11}B MAS NMR Spectra. The ^{11}B MAS NMR spectra of GTB x samples are shown in Figure 6. The spectra of $\text{B}(\text{OH})_3$ is also reported as a reference for a trigonal B surrounded by O atoms. For $\text{B}/\text{Si} \leq 0.3$, the three spectra present rather similar broad signals, ranging between 0 and 30 ppm and characteristic of tricoordinated B atoms. If one compares these spectra with that of $\text{B}(\text{OH})_3$, one can notice that the signals for GTB x samples extend over a larger range of chemical shift

values up to 35 ppm. Such high chemical shift values are unusual for BO_3 sites and agree more with BCO_2 sites. A value of 31.5 ppm has been reported from $\text{EtB}(\text{OME})_2$.²¹ For $\text{B}/\text{Si} \geq 0.5$, the sharp peak, detected at 0 ppm, is assigned to tetracoordinated BO_4 units. The broader peak around 15 ppm is, instead, assigned to trigonal BO_3 units.

Discussion

Epoxy Ring Opening. The opening of the epoxy rings in GPTMS-derived silane moieties involves different complex reactions. This opening reaction is efficiently catalyzed by BF_3 , but however can occur in some extents also in the absence of BF_3 or any other specific catalyst. The cleavage of epoxy groups with water, in acidic conditions, with the formation of diols, is a well-known reaction⁹ that has already been observed in sol-gel synthesis of GPTMS-derived hybrid materials. If this reaction occurs, the epoxy ring is cleaved but the formation of a poly(ethylene oxide) chain is inhibited (Scheme 4). This reaction should be, therefore, controlled if organic polymerization is the desired reaction.

Nor FTIR spectra, neither ^{13}C CP MAS NMR spectra show clear evidence for signals that can be attributed to residual diols in the hybrid network. This suggests that even if the hydrolysis of the epoxy rings under our synthesis conditions is possible, the reaction of BF_3 with the epoxy ring is much faster so that extensive organic polymerization is easily achieved.

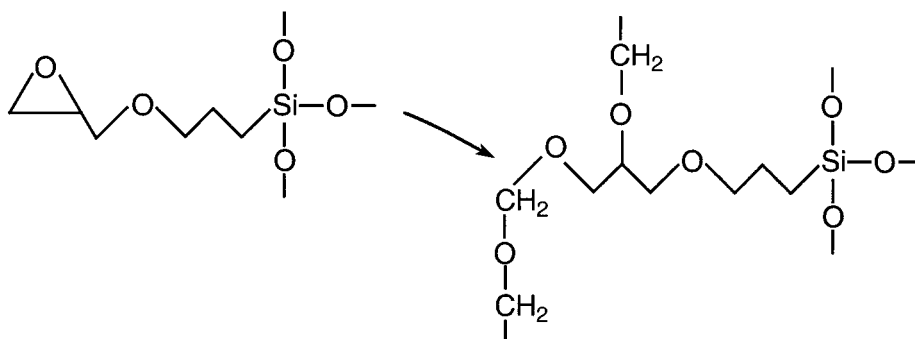
Another possible reaction involving the opening of epoxy in the absence of specific catalysts is the reaction of epoxy with methanol⁹ (Scheme 3).

Methanol is the solvent used in the present synthesis and it can react with the oxiranes to give methyl ether terminal groups (Figure 4). Up to a $\text{B}/\text{Si} = 0.3$, no significative difference in the amount of methyl ether units is observed. The difference found in GTB5 and GTB10 (Figure 4) is indeed due to the effect of large amounts of BF_3 on the polymerization of inorganic network, as it will be specifically discussed later on.

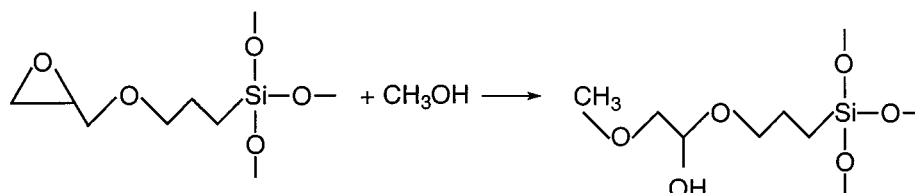
Templin and co-workers⁹ estimated that by employing aluminum butoxide in the synthesis of hybrids from GPTMS, at least 25% of the epoxy groups is reacting with methanol or water, which led to the conclusion that mainly oligoethylene derivatives are present in these hybrid materials. A comparison of the ^{13}C CP MAS NMR spectra of GPTMS-based samples in which the epoxy ring opening has been catalyzed either by BF_3 (Figure 4) or by aluminum alkoxide⁹ shows that the

(21) Nöth, H.; Vahrenkamp, H. *Chem. Ber.* **1966**, *99*, 1049.

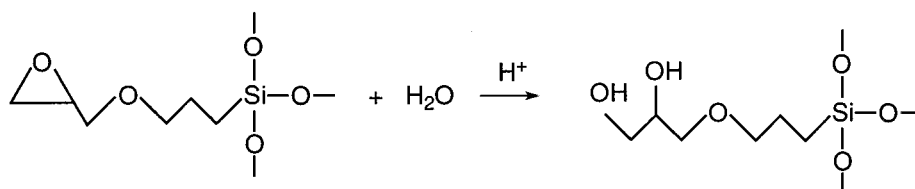
Scheme 2



Scheme 3



Scheme 4



synthesis by BF_3 is much more efficient to avoid the formation of diols and to obtain a larger organic polymerization. It is important to observe that in the GTB3 sample a complete ring opening is already achieved with no significant amount of residual diols. A consequence of the epoxide opening is the formation of oligo- or poly-(ethylene oxide) units.⁹ The terminal groups of these chains can be methyl ether units, as previously discussed, or even ethyl ether units. Ethanol is formed from the hydrolysis of TEOS and can react with the cleaved epoxy rings. However, because of the low amount of ethanol in the sol, this reaction is certainly very limited as no ethyl ether signals can be seen in the ^{13}C CP MAS NMR spectra (Figure 4).

Formation of Si–O–B Bonds. The elemental analysis of the powders (Table 1) confirms that boron remains in the final samples; the differences observed with respect to the nominal composition may be due to experimental error during the synthesis or to a loss of volatile species containing boron during synthesis. Solid-state NMR and FTIR results point out an important feature regarding the boron species in the final network: the boron introduced with BF_3 to catalyze the epoxy ring opening indeed behaves also as a network former. The FTIR spectra show the formation of Si–O–B bonds in the matrix (Figure 2). It was impossible to confirm that on the basis of the NMR results. As already reported in the literature,²² there is no ^{29}Si chemical shift differences between $\equiv\text{Si}-\text{O}-\text{Si}\equiv$ and

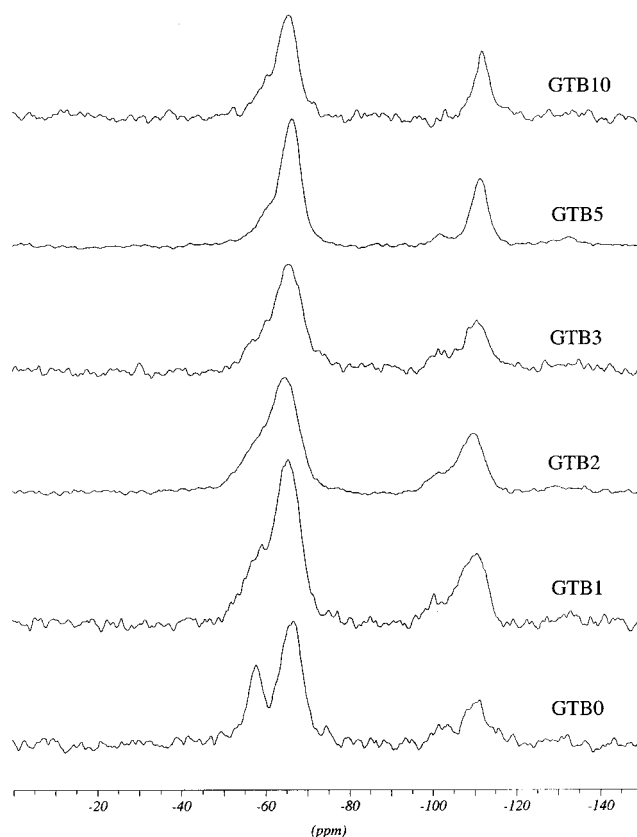


Figure 5. ^{29}Si MAS NMR spectra of the samples prepared with different amounts of BF_3 .

$\equiv\text{Si}-\text{O}-\text{B}\equiv$. Identification of such bonds has already been reported for similar organically modified silicates,

(22) (a) Irwin, A. D.; Holmgren, J. S.; Jonas, J. *J. Non-Cryst. Solids* **1986**, *83*, 208. (b) Bunker, B.; Tallant, D. R.; Kirkpatrick, R. J.; Turner, G. L. *Phys. Chem. Glasses* **1990**, *31*, 30.

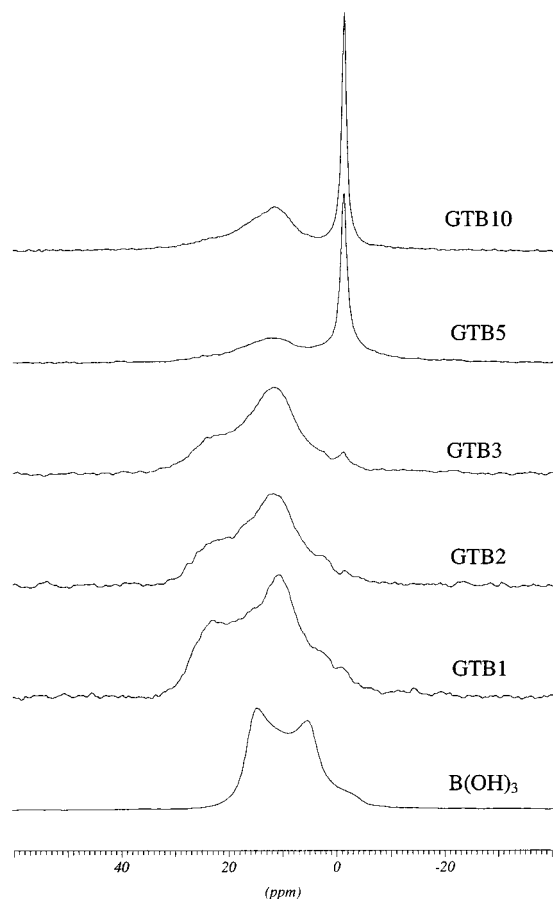


Figure 6. ^{11}B MAS NMR spectra of the samples prepared with different amounts of BF_3 . The $\text{B}(\text{OH})_3$ spectra is reported for reference.

Table 3. Results of the Simulation of ^{29}Si MAS NMR Spectra of Figure 5

sample	T:Q	T units		Q units	
		$T_2/(T_2 + T_3)$		$Q_3/(Q_3 + Q_4)$	
GTB0	77:23	0.33		0.20	
GTB1	73:27	0.30		0.29	
GTB2	72:28	0.24		0.17	
GTB3	71:29	0.16		0.17	
GTB5	70:30	0.16		0.07	
GTB10	72:28	0.22		0	

using ^{11}B MAS NMR.²³ But in the present case, it is rather difficult to describe the boron environment in the matrix. The ^{11}B MAS NMR spectra show a definite change in the coordination state of the boron atoms. Up to $\text{B}/\text{Si} = 0.3$, the signal is mainly due to tricoordinated boron atoms. The shape of the resonance signal is different from that of $\text{B}(\text{OH})_3$ (Figure 6), but does not exhibit clear discontinuities that could help in the analysis. It is characteristic of a distribution of boron sites in the matrix, with possibly some BCO_2 units, which suggests the formation of $\text{B}-\text{C}$ bonds. Above $\text{B}/\text{Si} = 0.5$, boron atoms are also tetraordinated with a relative ratio, $\text{B}(\text{IV}):\text{B}(\text{III}) = 60:40$. The reason for the formation of the tetrahedral boron environment is currently unknown.

Effect of BF_3 on Inorganic Polymerization. Using BF_3 in the synthesis affects not only the organic polym-

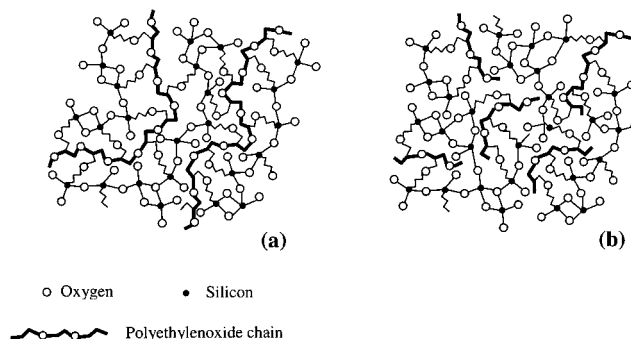


Figure 7. Schematic representation of the network that is formed when little (a) or large amounts (b) of BF_3 are employed.

erization but also the formation of the inorganic silica network. The shift to larger wavenumbers of the IR absorption peak around 1100 cm^{-1} due to $\text{Si}-\text{O}-\text{Si}$ vibrations (Figure 3) with larger BF_3 amounts is an indication of an increased strengthening of the matrix. This effect on the inorganic network is much stronger in these samples, prepared by BF_3 , than in the other hybrids based on GPTMS and prepared with different types of Lewis acids, as demonstrated in a previous paper.¹³ The catalytic effect of BF_3 on the reaction of the silicon alkoxide is clearly shown by ^{29}Si MAS NMR spectra (Figure 6 and Table 3). Larger amounts of BF_3 , indeed, reduce and even suppress the signal of T_2 and Q_3 units. Another indication is also given by the broadening of the ^{13}C resonance signals of the C atoms close to silicon with increasing BF_3 contents (Figure 4). This broadening is in fact due to the packing of these units in different environments and is related to a structural restricted mobility.

Competitive Polymerization. BF_3 , as previously shown, plays a double role, the first for the epoxy ring opening and poly(ethylene oxide) polymerization and the second for the inorganic network formation. These two processes, however, can be competitive with respect to each other. The ^{13}C MAS-NMR spectra in Figure 4 show that when larger boron contents are used, the amount of terminal methyl ether units increases. This is, however, accompanied by an increased inorganic network strength. The large amount of BF_3 has in fact the effect to increase the condensation of $\text{Si}-\text{OR}$ and $\text{Si}-\text{OH}$ groups to form a $\text{Si}-\text{O}-\text{Si}$ network. If the silica network grows faster than the organic chains, there will no longer be enough space to form poly(ethylene oxide) chains, and this will lead to the formation of oligomeric species as a result of sterical restriction. This effect is schematically represented in Figure 7. Figure 7a shows a network where the synthesis conditions favor the formation of longer poly(ethylene oxide)s chains, while in Figure 7b, the fast and extensive polymerization of the inorganic side hinders the growth of the organic network.

The possibility to have oligo- or polyethylene units is, therefore, dictated by the specific conditions of synthesis. The type of catalyst and its relative amount employed in the preparation affect the formation of the inorganic as well as the organic networks of the hybrid material. In general, this effect should be taken into account in the design of hybrid materials where organic and inorganic species can simultaneously polymerize.

(23) Sorarù, G. D.; Dallabona, N.; Gervais, C.; Babonneau, F. *Chem. Mater.* **1999**, *11*, 910.

Conclusions

Hybrid organic–inorganic materials based on 3-glycidoxypropyltrimethoxysilane have been synthesized using different amounts of BF_3 etherate.

BF_3 has been found to act as a strong catalyst of inorganic Si–O–Si network formation and at the same time to catalyze the organic polymerization from an epoxy ring opening. Large amounts of BF_3 favor a fast and extensive polymerization of the inorganic side,

hindering the formation of long organic polymers. Low amounts of BF_3 , instead, allow the formation of poly-(ethylene oxide) derivatives.

The polymerization of organic and inorganic units in this class of hybrid materials results in a competitive process that is controlled by the type and amount of catalyst employed during the synthesis.

CM001139B